

# NADPH oxidase 5 has a crucial role in cellular motility of colon cancer cells

NAOKI ASHIZAWA<sup>1</sup>, HIROKI SHIMIZU<sup>1,2</sup>, KATSUTOSHI SHODA<sup>1</sup>, SHINJI FURUYA<sup>1</sup>,  
HIDENORI AKAIKE<sup>1</sup>, NAOHIRO HOSOMURA<sup>1</sup>, YOSHIHIKO KAWAGUCHI<sup>1</sup>,  
HIDETAKE AMEMIYA<sup>1</sup>, HIROMICHI KAWAIDA<sup>1</sup>, MAKOTO SUDO<sup>1</sup>, SHINGO INOUE<sup>1</sup>,  
HIROSHI KONO<sup>1</sup>, KEITA KATSURAHARA<sup>2</sup>, ATSUSHI SHIOZAKI<sup>2</sup> and DAISUKE ICHIKAWA<sup>1</sup>

<sup>1</sup>First Department of Surgery, Faculty of Medicine, University of Yamanashi, Chuo 409-3898;

<sup>2</sup>Division of Digestive Surgery, Department of Surgery, Kyoto Prefectural University of Medicine, Kyoto 602-8566, Japan

Received September 24, 2020; Accepted June 11, 2021

DOI: 10.3892/ijo.2021.5243

**Abstract.** NADPH oxidases (NOXs) are a family of transmembrane proteins that generate reactive oxygen species. It was previously reported that patients with colon cancer who had high NOX5 expression had poor prognosis. However, no studies have investigated the cellular functions of NOX5 in colon cancer. The present study aimed to clarify the relationship between NOX5 and cancer development using an *in vitro* model. Reverse transcription-quantitative PCR was performed to determine the NOX5 expression levels of colon cancer cell lines. NOX5-knockdown experiments were conducted, and the effect on cell proliferation, migration, and invasion were analyzed. In addition, mRNA microarray was conducted to assess changes in gene profile. NOX5 mRNA expression was high in HCT116 cells and moderate in SW48 cells. NOX5 knockdown significantly inhibited cell migration and invasion in both HCT116 and SW48 cells; however, NOX5 knockdown reduced cell proliferation in only HCT116 cells. mRNA microarrays revealed a strong relationship between NOX5 expression levels and integrin-linked kinase signaling pathways. The NOX5 expression in colon cancer cells affected cancer progression, especially cell motility. NOX5 may be a novel therapeutic target for the future development of treatments for colon cancer.

## Introduction

Reactive oxygen species (ROS) can damage DNA, lipids, and proteins, and the accumulated oxidative damages play

key roles in the development of diseases, such as hypertension, arteriosclerosis, arthritis, neurodegenerative disease and cancer (1). In addition, ROS can serve as messengers and can lead to the upregulation of several signaling pathways such as the growth factor kinase (2,3), Src/Abl kinase (4), and MAPK (5) pathways. These specific signaling pathways can activate several cancer-related transcription factors, such as activator protein 1 and nuclear factor- $\kappa$ B (6). NADPH oxidases (NOXs) are a family of transmembrane proteins that generate ROS through the transmission of electrons across membranes. Seven isoforms of NOXs, including NOX1-5 and DUOX1-2, have been identified to date (7). These NOXs differ in organ expression, type of ROS produced, and the activation mechanism. NOXs are activated by a cytosolic activator or through the elevation of intracellular calcium ion levels. In the present study, focus was placed on NOX5, which is activated by the elevation of intracellular calcium ion levels (7). NOXs have physiological functions and are also associated with several chronic diseases, such as cardiovascular disease (8), neurodegenerative disease (9), inflammatory bowel disease (10), and pulmonary fibrosis (11). Additionally, NOXs have been reported to be associated with various types of cancer, including colon (12), gastric (13), pancreas (14), lung (15), and prostate (16) cancer.

NOX5 has been linked to malignant diseases such as prostate cancer (16), breast cancer (17), melanoma (18), hairy cell leukemia (19), and esophageal cancer (20). It was previously reported that patients with colon cancer with high NOX5 expression had significantly poor prognosis (21). However, no study has examined the physiological cellular functions of NOX5 in cancer progression. In the present study, functional analyses were conducted using an *in vitro* model to determine the relationship between NOX5 expression and cancer development, specifically for colon cancer.

## Materials and methods

**Cell culture, antibodies and other reagents.** Two human colon cancer cell lines, HCT116 and SW48, were purchased from RIKEN BioResource Center and Cell Resource Center for Biochemical Research (KAC Co., Ltd.), respectively. Cell

---

**Correspondence to:** Dr Hiroki Shimizu, Division of Digestive Surgery, Department of Surgery, Kyoto Prefectural University of Medicine, 465 Kajii-cho Road, Kyoto 602-8566, Japan  
E-mail: hiro0810@koto.kpu-m.ac.jp

**Abbreviations:** NOX, NADPH oxidase; ROS, reactive oxygen species; ILK, integrin-linked kinase

**Key words:** NOX, colon cancer, cellular motility, ILK signaling, ROS

authentication for these two cell lines was performed using short tandem repeat profiling. Five human colon cancer cell lines (RKO, SW620, SW480, DLD1, and HT29) were purchased from the American Type Culture Collection (ATCC). HCT116 and RKO cells were cultured in Dulbecco's modified Eagle's medium (DMEM) (Gibco; Thermo Fisher Scientific, Inc.) at 37°C. DLD-1 cells were cultured in RPMI-1640 medium (Gibco; Thermo Fisher Scientific, Inc.) at 37°C. HT29 cells were cultured in McCoy's 5A and minimal essential medium (Gibco; Thermo Fisher Scientific, Inc.) at 37°C, respectively. SW48, SW480, and SW620 cells were cultured in Leibovitz's L-15 medium (Gibco; Thermo Fisher Scientific, Inc.) in a CO<sub>2</sub>-free environment at 37°C. All culture media were supplemented with 10% fetal bovine serum (FBS) (Gibco; Thermo Fisher Scientific, Inc.) and 1% penicillin/streptomycin.

A polyclonal NOX5 antibody (product code ab191010; Abcam), a monoclonal integrin  $\alpha$ 2 antibody (product code ab133557; Abcam) and  $\beta$ -actin antibody (product code ab8227; Abcam) were used in the present study. A polyclonal NOX5 antibody (cat. no. orb100974-CF405M; Biorbyt Ltd.) was used to confirm the results of western blotting for NOX5 protein by the ab191010 antibody.  $\beta$ -actin was used as a loading control in western blotting.

**Immunohistochemistry.** The detailed method of immunohistochemistry has been previously described (21). Tumor tissue and normal colonic mucosa were obtained from a 75-year-old male patient who underwent curative surgery for colon (cecum) cancer at the University of Yamanashi Hospital. The present study was approved (approval no. of the institution: 1940) by the Ethics Committee of the University of Yamanashi Hospital (Chuo, Japan) and written informed consent was obtained from the patient. The tissue sections were incubated overnight at 4°C with the NOX5 antibody (1:100).

**Western blotting.** The expression levels of NOX5 were evaluated in 7 colon cancer cell lines using western blotting. Cells were lysed in Pierce RIPA buffer (Thermo Fisher Scientific, Inc.) using a protease/phosphatase inhibitor cocktail (Cell Signaling Technology, Inc.). The protein concentration was assessed using NanoDrop 2000 (Thermo Fisher Scientific, Inc.) by Warburg-Christian method. Cell lysates containing 4 mg/ml of total protein were separated using 4-12% sodium dodecyl sulphate-polyacrylamide gel electrophoresis (Invitrogen; Thermo Fisher Scientific, Inc.) and electrophoretically transferred to polyvinylidene difluoride membranes (MilliporeSigma). The mass of protein loaded per lane was 40  $\mu$ g. Nonspecific binding was blocked using the same amount of Odyssey blocking buffer (LI-COR Biosciences) and phosphate-buffered saline at room temperature for 90 min. The membranes were probed with the indicated primary antibodies at 4°C for 16 h. Each primary antibody was diluted as follows: Anti-NOX5 antibody (Abcam) (1:1,000), anti-NOX5 antibody (Biorbyt) (1:500), anti-integrin  $\alpha$ 2 antibody (Abcam) (1:10,000), and anti- $\beta$ -actin antibody (Abcam) (1:5,000). Then, the membranes were incubated with HRP conjugated anti-rabbit secondary antibody (1:2,000 dilution; product code ab6721; Abcam) at room temperature for 1 h. The proteins were visualized using Pierce™ ECL Plus western blotting substrate (Thermo Fisher Scientific, Inc.), and the intensity of

the bands was assessed using ImageJ software version 1.8.0 (National Institutes of Health).

**Small interfering RNA (siRNA) transfection.** HCT116 and SW48 cells were transfected with 10 nmol/l NOX5 small interfering (si)RNA (Stealth siRNA Assay ID HSS128403; Invitrogen; Thermo Fisher Scientific, Inc.) using Lipofectamine RNAi MAX Transfection Reagent (Invitrogen; Thermo Fisher Scientific, Inc.) according to the manufacturer's protocol. In detail, 4  $\mu$ l of Lipofectamine RNAi MAX Transfection Reagent was diluted in 250  $\mu$ l of Opti-MEM I Reduced-Serum Medium (Gibco; Thermo Fisher Scientific, Inc.) and incubated at room temperature for 5 min. The medium containing siRNA was replaced with fresh medium 24 h after transfection. The Stealth RNAi™ siRNA Negative Control Med GC Duplex #2 (cat. no. 12935112; Invitrogen; Thermo Fisher Scientific, Inc.) was used as a negative control siRNA (10 nmol/l). At 48 h after transfection, total RNA was extracted from the cells and purified using the miRNeasy Mini Kit (Qiagen GmbH) following the manufacturer's instructions.

**Reverse transcription-quantitative PCR (RT-qPCR).** Total RNA was purified from the HCT116, SW48, RKO, SW620, SW480, DLD1, and HT29 cells using the RNeasy Mini Kit (Qiagen GmbH) following the manufacturer's instructions. The concentration and purity of RNA were assessed using NanoDrop 2000. Absorbance was measured at wavelengths of 280, 260, and 230 nm. cDNA was synthesized using the high-capacity cDNA reverse transcription kit (Applied Biosystems™; Thermo Fisher Scientific, Inc.) according to the manufacturer's instructions. Quantitative PCR analysis was performed in 20- $\mu$ l reaction systems containing 2  $\mu$ l of cDNA, 1  $\mu$ l of appropriate primer, 10  $\mu$ l of TaqMan Universal PCR Master Mix (Applied Biosystems™; Thermo Fisher Scientific, Inc.), and 7  $\mu$ l of RNase-free water on a 96-well plate. The expression levels were evaluated for the following human genes: NOX5 (Hs00225846\_m1), Jun proto-oncogene (JUN) (Hs01103582\_s1), FBJ murine osteosarcoma viral oncogene homolog (FOS) (Hs00170630\_m1), plasminogen activator urokinase (PLAU) (Hs01547054\_m1), glycogen synthase kinase 3 $\beta$  (GSK3B) (Hs01047719\_m1), and integrin subunit  $\alpha$ 2 (ITGA2) (Hs00158127\_m1) (Thermo Fisher Scientific, Inc.). GAPDH (cat. no. 4310884E; Applied Biosystems™; Thermo Fisher Scientific, Inc.) was used as an endogenous control for normalization. RT-qPCR was performed using Applied Biosystems 7500 Real-Time PCR software (7500 Software version 2.0.6; Applied Biosystems™; Thermo Fisher Scientific, Inc.). The comparative cycle threshold (Cq) ( $\Delta\Delta$ Cq) method was used to analyze the data (22). The PCR thermocycling conditions were as follows: 2 min at 50°C, 10 min at 95°C, 40 cycles of 15 sec at 95°C and 1 min at 60°C. For quantification, the threshold cycle (Cq) was defined as the PCR cycle number. Each assay was performed in triplicate.

**Cell proliferation assay and cell cycle analysis.** Cells were seeded at a density of 0.5x10<sup>5</sup> cells/ml in a 6-well plate and incubated at 37°C with 5% CO<sub>2</sub>. siRNA transfection was performed 24 h after seeding. At 24, 48, and 72 h after transfection, the cells were dislodged using 0.53 mmol/l trypsin-EDTA solution (Nacalai Tesque Inc.), and the cells were counted using

Countess Automated Cell Counter (Invitrogen™; Thermo Fisher Scientific, Inc.). Each assay was performed in triplicate. The cell cycle was evaluated using fluorescence-activated cell sorting (FACS) (BD FACSDiva software version 8.0; BD Biosciences) as previously described (23). Briefly, the cells were detached using trypsin-EDTA solution and treated with Triton X-100 and RNase. The nuclei were stained for 15 min at room temperature with propidium iodide. Thereafter, the DNA content was assessed using FACS with analysis of at least  $2 \times 10^4$  cells.

**Cell migration, invasion and wound healing assays.** A migration assay was conducted in a 24-well Transwell system with control chambers of 8- $\mu$ m pore size (product no. 353097; Corning, Inc.) and an invasion assay in a 24-well Transwell system with Matrigel chambers of 8- $\mu$ m pore size (product no. 354480; Corning, Inc.). The Matrigel was incubated to rehydrate at 37°C for 2 h. HCT116 and SW48 cells were seeded at densities of  $1.5 \times 10^5$  and  $3.0 \times 10^5$  cells/ml in the upper chambers, respectively, at 24 h after siRNA transfection. The upper chamber was filled with 0.75 ml of serum-free medium, and the lower chamber was filled with 0.5 ml of medium supplemented with 10% FBS. At 48 h for the migration assay and 60 h for the invasion assay after incubation at 37°C with 5% CO<sub>2</sub>, the cells that did not permeate the chamber were removed using a cotton swab, and the cells that were able to permeate the chamber were stained with Differential Quik III Stain Kit (5% eosin Y and 5% azure-2) (Polysciences, Inc.) for each 30 sec at room temperature and counted with cell count software (ver. 2.2; Keyence Corporation) using a light microscope. Ibidi culture inserts (Ibidi GmbH) were used for the wound healing assay. This assay was started with 100% confluent HCT116 cells. HCT116 cells were detached at 48 h after siRNA transfection, and  $8.0 \times 10^6$  cells/70  $\mu$ l were seeded in each area. After 24 h, the insert was removed and each well was filled with the medium with 10% FBS. Images of the migrated cells were captured at 24 h after removing the insert using phase-contrast microscope, and the rate of gap closure was analyzed with cell count software (ver. 2.2). Each assay was performed in triplicate.

**Gene microarray analysis.** HCT116 cells were transfected with control siRNA (n=1) and NOX5 siRNA (n=1). Total RNA was extracted from the cells using a miRNeasy Mini Kit (Qiagen GmbH) according to the manufacturer's protocol at 48 h after transfection. The RNA quality was assessed using NanoDrop 2000 (Thermo Fisher Scientific, Inc.) and Agilent 2100 Bioanalyzer (Agilent Technologies, Inc.). Microarray analyses were performed with a 3D-Gene Human Oligo chip 25k (Toray Industries, Inc.). This microarray adopted a columnar structure to stabilize spot morphology and enable microbead agitation for efficient hybridization. Total RNA was labeled with Cy5 or Cy3 using the Amino Allyl MessageAMP II aRNA Amplification Kit (Applied Biosystems; Thermo Fisher Scientific, Inc.). The Cy5- or Cy3-labeled aRNA pools were mixed with hybridization buffer, and subsequently hybridized for 16 h. The hybridization was performed according to the manufacturer's protocols ([www.3d-gene.com](http://www.3d-gene.com)). The hybridization signals were acquired using a 3D-Gene Scanner (Toray Industries, Inc.) and processed using 3D-Gene Extraction

software (ver.1.2.1.1; Toray Industries, Inc.). The detected signals for each gene were normalized using a global normalization method (Cy3/Cy5 ratio median=1). The fold change of each molecule was calculated by the normalized data of two samples, and a fold change cutoff value of two or three times or more was set to identify significantly downregulated molecular expressions. The network and pathway analyses were performed using Ingenuity Pathway Analysis (IPA) (ver. 62089861; Ingenuity Systems; Qiagen). Molecules were represented by nodes, and the biological relationship between two nodes was represented as an edge. The functional analysis was identified along with biological function and diseases. The microarray data used in the present study have been deposited in the Gene Expression Omnibus (GEO; <http://www.ncbi.nlm.nih.gov/geo/>) of NCBI and are accessible through GEO Series accession number GSE175691.

**Measurement of extracellular hydrogen peroxide.** The level of extracellular hydrogen peroxide (H<sub>2</sub>O<sub>2</sub>) was assessed using the Amplex Red Hydrogen Peroxidase Assay kit following the manufacturer's instructions (Invitrogen™; Thermo Fisher Scientific, Inc.). Briefly, the reaction mixture contained 50  $\mu$ M Amplex Red reagent, 0.1 U/ml HRP, and 5  $\mu$ M ionomycin (Merck KGaA) in Krebs-Ringer phosphate glucose (KRPBG) and was incubated for 10 min at 37°C. At 48 h after siRNA transfection, HCT116 and SW48 cells were detached and 20  $\mu$ l of  $2.0 \times 10^4$  cells were suspended in KRPBG buffer and added to the prepared reaction mixture. Fluorescence was assessed using a fluorescence microplate reader at an excitation wavelength of 530 nm and fluorescence detection at 590 nm. The absorbance was measured at 1 and 3 h after the cells were added to the reaction mixture.

**Statistical analysis.** The results were expressed as the mean  $\pm$  standard error of the mean from at least three experiments. The data were analyzed using JMP statistical software (version 14.2; SAS Institute, Inc.). Unpaired Student's t-test was used to assess statistical differences between mean values of control and treated samples.  $P < 0.05$  was considered to indicate a statistically significant difference.

## Results

**Expression levels of NOX5 in human colon cancer cell lines.** The expression levels of NOX5 mRNA and protein in 7 colon cancer cell lines were examined to investigate the role of NOX5 in cancer development. NOX5 mRNA was highly expressed in HCT116 cells, moderately expressed in DLD1, SW48, and SW480 cells, and lowly expressed in HT29, RKO, and SW620 cells (Fig. 1A). NOX5 protein expression could be detected at various levels in all cell lines (Fig. 1B). NOX5 protein expression could be detected with similar levels using another anti-NOX5 antibody (Fig. S1A and B). Using human colon cancer tissues, immunohistochemical staining demonstrated weaker NOX5 expression levels in the normal colonic mucosa than in the tumor tissues (Fig. 1C and D).

**Limited effect of NOX5 on cell proliferation in colon cancer cells.** Further examination was conducted on HCT116 and SW48 cells. DLD1 cells, another cell line with a moderate

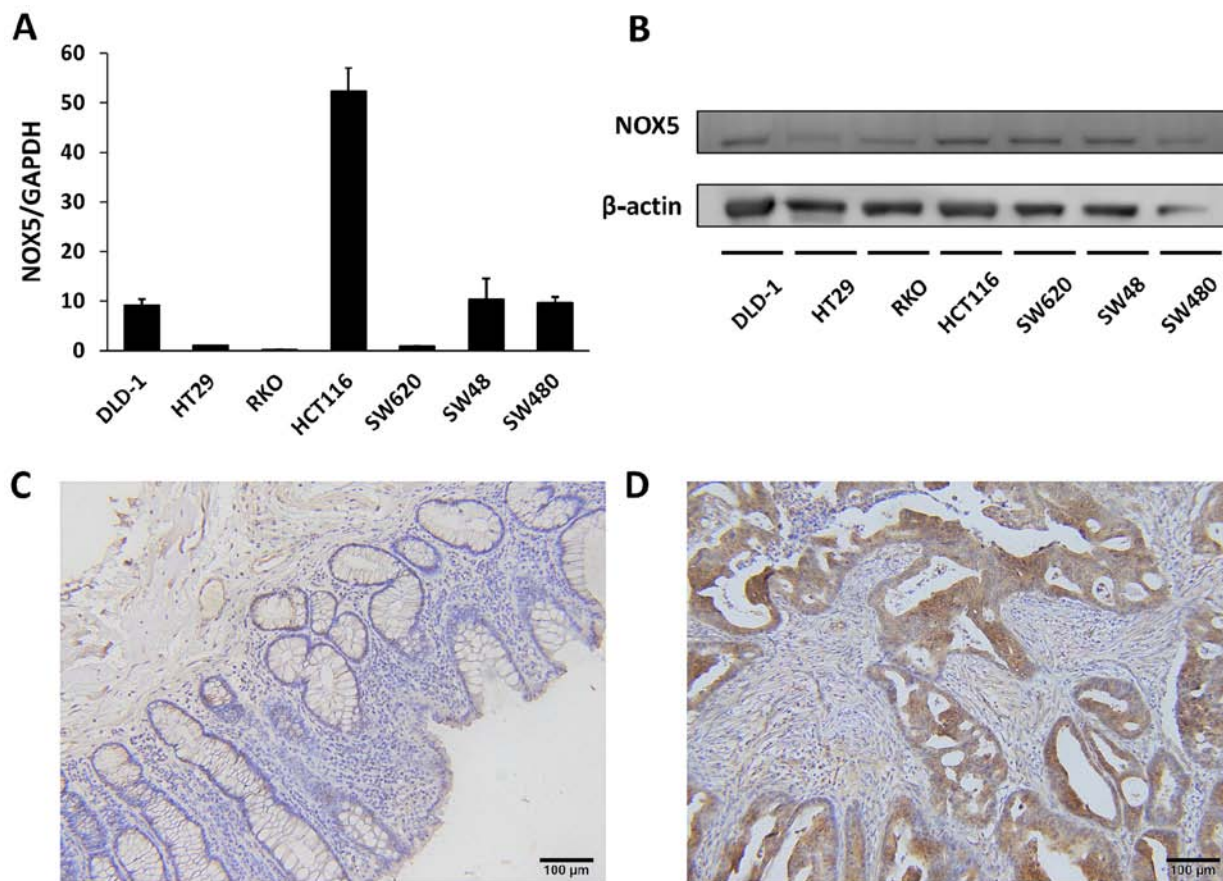


Figure 1. Expression of NOX5 mRNA and protein in colon cancer cells. (A) NOX5 mRNA was highly expressed in HCT116 cells and moderately expressed in DLD1, SW48, and SW480 cells. (B) NOX5 protein was highly expressed in HCT116 cells and moderately expressed in SW48 cells. (C and D) Immunohistochemical staining for NOX5 protein using human colon tissue. (C) NOX5 protein was lowly expressed in the normal colonic mucosa. (D) NOX5 protein was highly expressed in the tumor tissue. Data are expressed as the mean  $\pm$  SEM.  $n=3$ . NOX, NADPH oxidase.

level of NOX5 expression, was not selected due to the low efficiency of NOX5 knockdown according to the result of RT-qPCR ( $0.51 \pm 0.06$ ; data not shown). NOX5 siRNA transfection effectively downregulated NOX5 mRNA expression in both cell lines (Fig. 2A) and NOX5 protein expression in HCT116 cells (Fig. 2B). In HCT116 cells, the downregulation of NOX5 expression led to a significantly lower number of viable cells at 48 ( $P=0.013$ ) and 72 h ( $P<0.001$ ) after transfection, whereas there was no difference in the number of cells at these time-points for SW48 cells (Fig. 2C). Cell cycle analysis also revealed that downregulation of NOX5 expression led to G<sub>2</sub>/M arrest only in HCT116 cells, which supported the results of the cell proliferation assay (Fig. 2D).

**NOX5 regulates cell migration and invasion in colon cancer cells.** The role of NOX5 in cancer progression was further explored. The migrated and invasive cell number ratio of NOX5-knockdown cells was significantly reduced to  $13.2 \pm 1.2$  and  $36.3 \pm 4.3\%$  in HCT116 cells ( $P<0.01$  and  $P<0.01$ , respectively) (Fig. 3A). Similarly, the migrated and invasive cell number ratio of NOX5-knockdown cells was significantly reduced to  $9.6 \pm 4.6$  and  $19.5 \pm 3.3\%$  compared with that in control SW48 cells ( $P<0.01$  and  $P=0.010$ , respectively) (Fig. 3B). The wound healing assay revealed that the horizontal cellular motility of NOX5-knockdown HCT116 cells was significantly inhibited ( $P<0.01$ ) (Fig. S2).

**Level of extracellular  $H_2O_2$  in HCT116 and SW48 cells.** To confirm the effect of NOX5 knockdown on ROS production, the level of extracellular  $H_2O_2$  in the culture medium of HCT116 and SW48 cells was assessed. The  $H_2O_2$  level was significantly increased by NOX5 knockdown in both HCT116 and SW48 cells (Fig. S3).

**Gene expression profiling in NOX5 siRNA-transfected cells.** A comprehensive analysis using mRNA microarray was performed to examine changes in the gene expression profiles of NOX5 siRNA-transfected HCT116 cells and control siRNA-transfected HCT116 cells. The microarray analysis revealed a total of 4,043 genes with changes of  $\geq 1.4$ -fold in HCT116 cells subjected to NOX5 knockdown. Of these genes, 2,323 were upregulated and 1,720 were downregulated. IPA analysis revealed that cancer was one of the top-ranked diseases and that integrin-linked kinase (ILK) signaling was one of the top-ranked canonical pathways related to NOX5 knockdown (Table I; Fig. 4).

**Verification of microarray results.** A total of five genes related to the ILK signaling pathway (*ITGA2*, *GSK3B*, *JUN*, *FOS* and *PLAU*) were selected to confirm the results of the microarray analysis (Table II; Fig. 4). The expression levels of these genes were analyzed using RT-qPCR. The expression levels of each gene were compared between NOX5

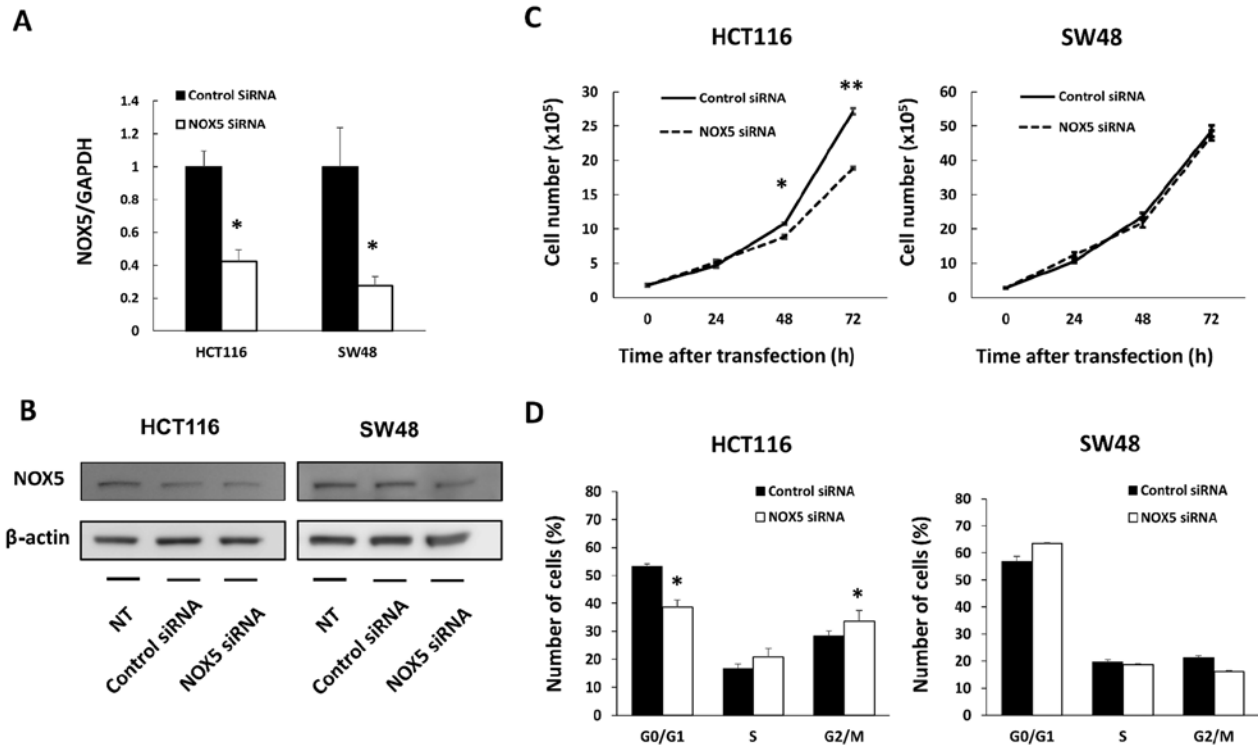


Figure 2. Depletion of NOX5 significantly inhibits cell proliferation and cell cycle progression in HCT116 cells but not in SW48 cells. (A) mRNA expression of NOX5 was significantly downregulated by depletion of NOX5. (B) Transfection with NOX5 siRNA downregulated the protein expression of NOX5. (C) Depletion of NOX5 significantly inhibited cell proliferation in HCT116 cells, but it had no effect on cell proliferation in SW48 cells. (D) Depletion of NOX5 reduced cell cycle progression from G<sub>2</sub>/M to G<sub>0</sub>/G<sub>1</sub> phase in only HCT116 cells. Data are expressed as the mean ± SEM. n=3 (A, C and D). \*P<0.05 and \*\*P<0.01. NOX, NADPH oxidase; si, small interfering.

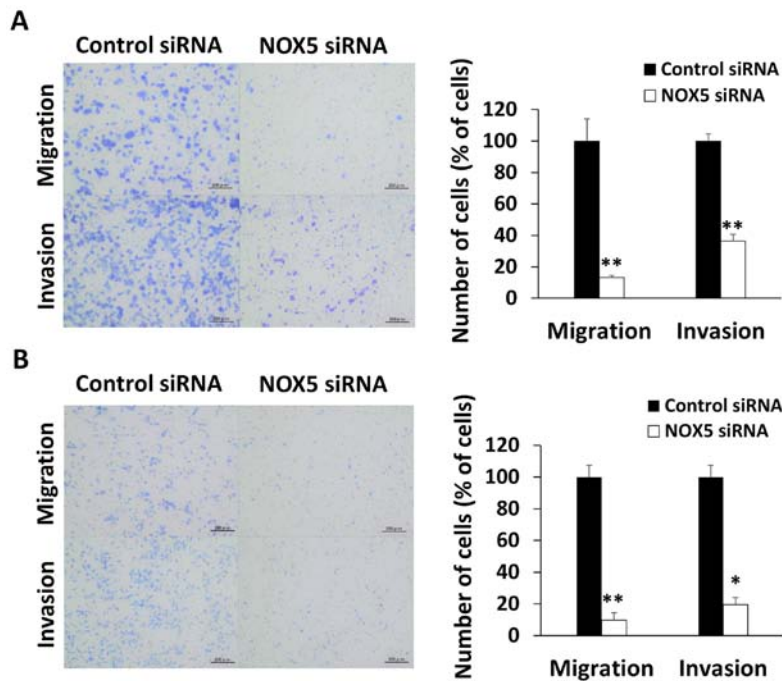


Figure 3. Depletion of NOX5 significantly inhibits cellular motility in two cell lines. (A) HCT116 cells and (B) SW48 cells. Data are expressed as the mean ± SEM. n=3. \*P<0.05 and \*\*P<0.01. NOX, NADPH oxidase; si, small interfering.

siRNA-transfected HCT116 cells and control siRNA-transfected HCT116 cells. NOX5 siRNA-transfected HCT116 cells revealed significantly decreased mRNA expression levels of *ITGA2*, *GSK3B*, *JUN*, *FOS*, and *PLAU* compared

with the control cells (Fig. 5A). The *ITGA2* protein level was also decreased by NOX5 siRNA-transfection (Fig. 5B). These changes were consistent with the results of the microarray analysis.

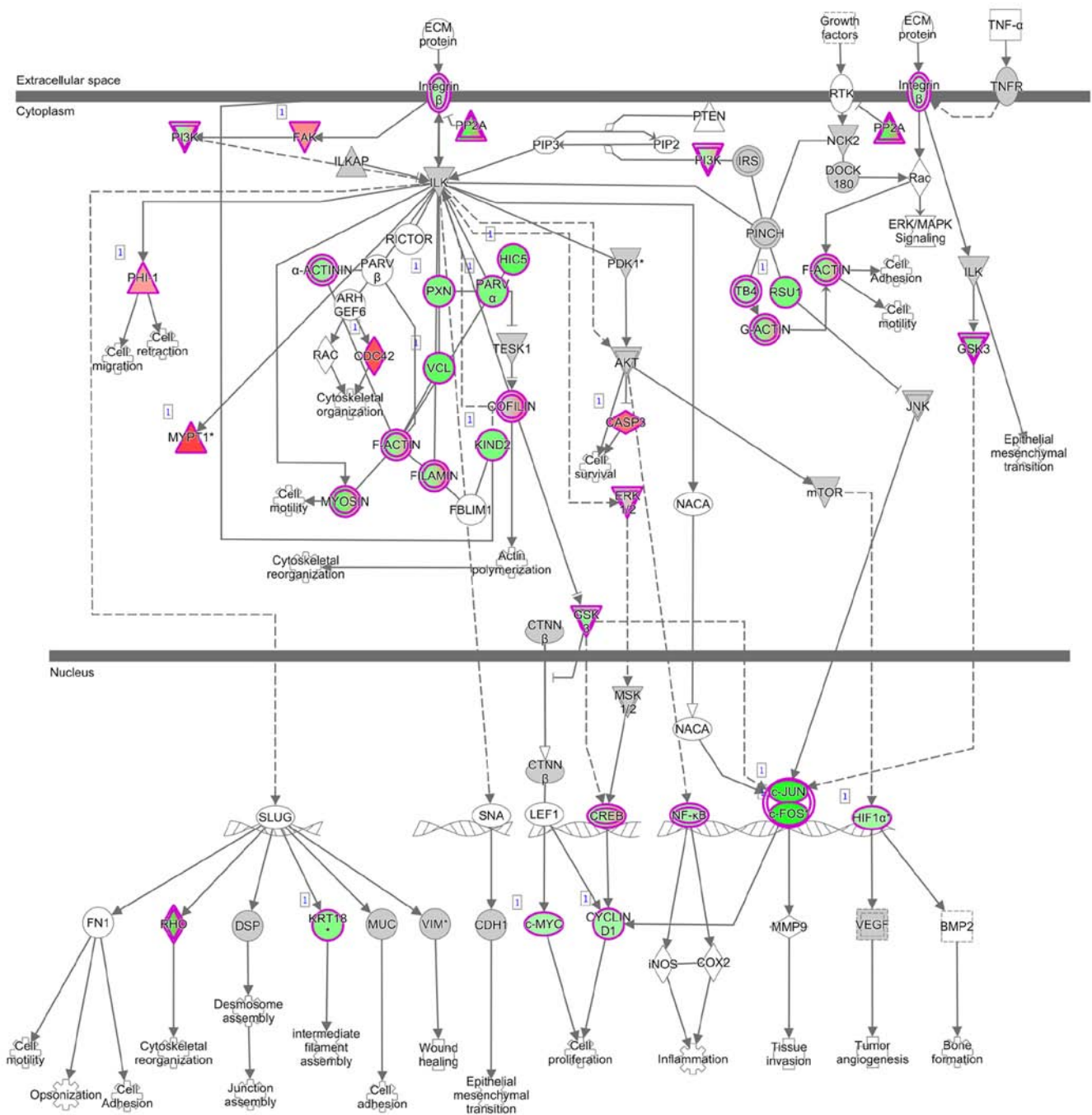


Figure 4. Map of integrin-linked kinase signaling according to Ingenuity Pathway Analysis. Red and green indicate genes whose expression levels were higher and lower than the reference RNA levels with changes of  $\geq 1.4$ -fold by the depletion of NOX5, respectively. NOX, NADPH oxidase.

## Discussion

The role of NOX5 in tumor progression of colon cancer was examined using human colon cancer cell lines. To the best of our knowledge, this is the first study involving *in vitro* experiments to determine the oncogenic role of NOX5 in colon cancer.

The NOX family is composed of seven members consisting of NOX1 to NOX5 and DUOX1 and 2, which generate ROS (24). There have been numerous studies concerning the roles of the NOX family in cancer. In colon cancer, NOX1 has been well studied and it has been reported that NOX1 is highly expressed in colon cancer and involved in cancer

progression (10,25,26). In addition, NOX4 was revealed to be involved in protecting pancreatic cancer cells from apoptosis by producing ROS (14). DUOX1 and DUOX2 have been revealed to increase cell migration in lung cancer (15). However, the functions of NOX5 have not been investigated thoroughly as NOX5 was the latest discovery among the members of the NOX family. It was only discovered in 2001. The NOX5 gene is located on chromosome 15, with four splice variants ( $\alpha$ ,  $\beta$ ,  $\delta$ , and  $\gamma$ ) of NOX5 and one truncated variant (NOX5s or NOX5e). NOX5 $\alpha$ , NOX5 $\beta$ , NOX5 $\delta$ , and NOX5 $\gamma$  are known as NOX5-L (27). NOX5 is known to be expressed in a variety of organs such as lymphatic tissues, testes (28), vascular smooth muscles (29), and kidneys (30).

Table I. Major NADPH oxidase 5 canonical pathways and disease/biological functions according to Ingenuity Pathway Analysis.

## A, Top canonical pathways

Name	P-value	Overlap
Protein ubiquitination pathway	$1.58 \times 10^{-9}$	30.8%
EIF2 signaling	$9.75 \times 10^{-8}$	30.4%
Molecular mechanisms of cancer	$2.19 \times 10^{-7}$	26.3%
Integrin-linked kinase signaling	$6.73 \times 10^{-7}$	30.5%
Regulation of actin-based motility by Rho	$7.21 \times 10^{-7}$	37.2%

## B, Top Diseases and Bio Functions (disease and disorders)

Name	P-value range	Molecules
Cancer	$1.57 \times 10^{-4}$ - $9.24 \times 10^{-143}$	3,488
Organismal injury and abnormalities	$1.57 \times 10^{-4}$ - $9.24 \times 10^{-143}$	3,516
Endocrine system disorders	$1.57 \times 10^{-4}$ - $1.75 \times 10^{-98}$	2,721
Gastrointestinal disease	$1.57 \times 10^{-4}$ - $1.99 \times 10^{-67}$	3,002
Reproductive system disease	$1.57 \times 10^{-4}$ - $7.16 \times 10^{-16}$	1,974

Table II. Expression level patterns of ILK signaling pathway-related genes in HCT116 cells after NADPH oxidase 5 knockdown.

Gene symbol	UniGene ID	ILK signaling pathway	
		Gene name	Fold change
<i>ITGA2</i>	H200016773	Integrin subunit $\alpha 2$	-2.51
<i>GSK3B</i>	H300019897	Glycogen synthase kinase 3 $\beta$	-2.04
<i>JUN</i>	opHsV0400001031	Jun proto-oncogene	-5.69
<i>FOS</i>	H200003548	FBJ murine osteosarcoma viral oncogene homolog	-4.50
<i>PLAU</i>	H300019040	Plasminogen activator, urokinase	-4.61

ILK, integrin-linked kinase.

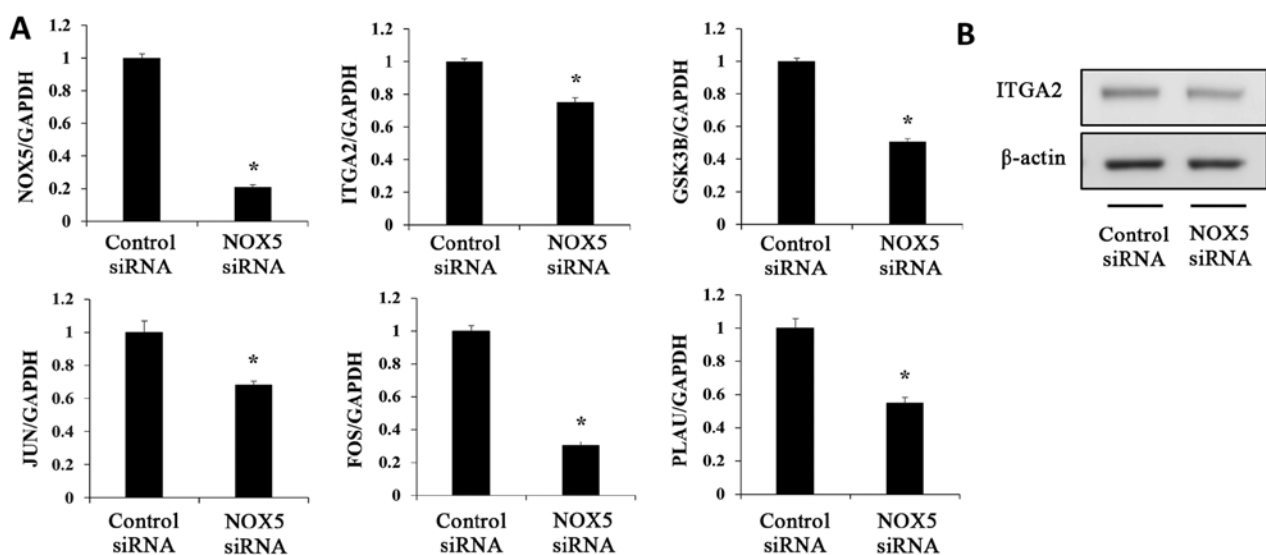


Figure 5. Verification of microarray results. (A) The mRNA expression of NOX5 and five selected genes related to integrin-linked kinase signaling pathway in NOX5 siRNA-transfected HCT116 cells were compared with those in control siRNA-transfected cells. The expression of each gene was normalized against that of GAPDH. (B) The ITGA2 protein level was decreased by NOX5 siRNA-transfected HCT116 cells. Data are expressed as the mean  $\pm$  SEM.  $n=3$ . \* $P<0.05$ . NOX, NADPH oxidase; si, small interfering; ITGA2, integrin subunit  $\alpha 2$ ; FOS, FBJ murine osteosarcoma viral oncogene homolog; JUN, Jun proto-oncogene; PLAU, plasminogen activator urokinase; GSK3B, glycogen synthase kinase 3 $\beta$ .

NOX5 has been revealed to regulate monocyte differentiation into dendritic cells in the immune system (31). NOX5 also plays a role in vascular contraction and is involved in the development of hypertension and atherosclerosis (32,33). In addition, NOX5 has been associated with various types of cancer. Previous studies have reported that NOX5 plays an important role in cancer growth, migration, and invasion in prostate (16), breast (17), and esophageal cancer (34) through signaling pathways, such as the MAPK pathway (35). However, the role of NOX5 in colon cancer remains unclear unlike NOX1 (12). NOX5 reportedly promotes cancer cell proliferation, migration, and invasion in breast cancer cell lines (17). The present study also demonstrated that NOX5 was involved in the tumor motility of colon cancer. With regard to the cell growth rate and cell cycle, different levels of NOX5 mRNA/protein expression in colon cancer cells were associated with the results of the present study. It was observed that the high levels of NOX5 expression in HCT116 cells played a role in the regulation of cell cycle progression and cell proliferation; however, SW48 cells only moderately expressed NOX5 and were not involved in the same mechanisms of cell cycle regulation and proliferation as those in which HCT116 cells were involved. It was previously reported that patients with colon cancer who had high NOX5 expression had significantly poor prognosis with high rates of metastasis after curative resection (21), which corroborates with the results of the present study.

ILK is a protein kinase that is attached to the integrin  $\beta$ -subunit, and the basic function of integrins is to promote cell-to-cell and cell-to-extracellular matrix adhesion and cell migration. ILK serves as an important regulator of signaling cascades, such as P13K/AKT, AP-1, Hippo, NF- $\kappa$ B, and ERK (36), and plays important roles in cell proliferation, invasion, and migration in various types of cancer. Furthermore, ILK is overexpressed in colon cancer tissues and is involved in epithelial-mesenchymal transition, metastasis and chemoresistance (37). In the present study, mRNA microarray experiments revealed that the expression levels of several genes involved in the ILK signaling pathway, such as ITGA2, GSK3B, JUN, and FOS, were significantly downregulated by the depletion of NOX5.

Plasminogen activator (PA) is a serine protease that comprises the plasminogen activator system, together with its plasminogen activator receptor and its inhibitor, plasminogen activator inhibitor (38). There are two types of PA: Tissue type plasminogen activator and PLAU. PLAU is mainly involved in cancer malignancies, including colorectal cancer (39-41). It has been reported that PLAU forms a complex with integrin and activates pathways such as the PTK2 and ERK pathways and is involved in cell proliferation and invasion (38,42). In the present study, both mRNA microarray and its validation experiments revealed that the depletion of NOX5 reduced PLAU expression. To the best of our knowledge, there has been no study in the cancer-related field on this topic, although there have been some studies that reported the relationship between NOX and integrins or PLAU in the noncancerous field (43,44). In addition, as the analysis of microarray results revealed that the expression levels of some Rho-related genes were also significantly altered (Table I), the Rho/ROCK signaling pathway may be another potential target and further study is necessary.

As it has previously been demonstrated that an increase in  $H_2O_2$  levels is associated with the triggering of cancer-related pathways in colorectal cancer (45,46), changes in extracellular  $H_2O_2$  levels were also evaluated by transfection with NOX5 siRNA. However, the extracellular  $H_2O_2$  levels did not decrease with NOX5 knockdown in both cell lines. These results indicated that other mechanisms are involved, and further studies are needed to clarify them. Although the lack of experiments in a normal colon cell line exists as a potential limitation, the present study demonstrated that changes in NOX5 expression could influence the ILK signaling pathway and PLAU expression on colon cancer development.

In conclusion, the present study revealed that NOX5 plays a role in cancer progression, especially on motility of cancer cells. Microarray data revealed that NOX5 knockdown influenced the expression of ILK signaling pathway-related genes. Our observations indicated that NOX5 may be a useful biomarker and a novel therapeutic target for the future treatment of colon cancer, although further investigation of the underlying molecular mechanism is necessary.

### Acknowledgements

Not applicable.

### Funding

The present study was supported by a Grant-in-Aid for Young Scientists (grant no. 20K17609) from the Japan Society for the Promotion of Science.

### Availability of data and materials

All data generated or analyzed during this study are included in this published article. The microarray data discussed in this publication have been deposited in the Gene Expression Omnibus (GEO, <http://www.ncbi.nlm.nih.gov/geo/>) of NCBI and are accessible through GEO Series accession number GSE175691.

### Authors' contributions

NA performed all experiments and wrote the manuscript. HS designed the project and wrote the manuscript. KS, SF, HAK, NH, YK, HAM, HKA, MS, SI, and HKO participated in the interpretation of the results and helped to edit the manuscript. KK and AS helped to analyze the results of microarray analysis. DI provided conceptual advice and edited manuscript. All authors read and approved the final version of the manuscript.

### Ethics approval and consent to participate

The present study was approved (approval no. of the institution: 1940) by the Ethics Committee of the University of Yamanashi Hospital (Kofu, Japan). Written informed consent was obtained from all patients.

### Patient consent for publication

Not applicable.

## Competing interests

The authors declare that they have no competing interests.

## References

- Valko M, Rhodes CJ, Moncol J, Izakovic M and Mazur M: Free radicals, metals and antioxidants in oxidative stress-induced cancer. *Chem Biol Interact* 160: 1-40, 2006.
- Bae YS, Kang SW, Seo MS, Baines IC, Tekle E, Chock PB and Rhee SG: Epidermal growth factor (EGF)-induced generation of hydrogen peroxide. Role in EGF receptor-mediated tyrosine phosphorylation. *J Biol Chem* 272: 217-221, 1997.
- Neufeld G, Cohen T, Gengrinovitch S and Poltorak Z: Vascular endothelial growth factor (VEGF) and its receptors. *FASEB J* 13: 9-22, 1999.
- Esposito F, Chirico G, Montesano Gesualdi N, Posadas I, Ammendola R, Russo T, Cirino G and Cimino F: Protein kinase B activation by reactive oxygen species is independent of tyrosine kinase receptor phosphorylation and requires SRC activity. *J Biol Chem* 278: 20828-20834, 2003.
- Kyriakis JM and Avruch J: Mammalian mitogen-activated protein kinase signal transduction pathways activated by stress and inflammation. *Physiol Rev* 81: 807-869, 2001.
- Hsu TC, Young MR, Cmarik J and Colburn NH: Activator protein 1 (AP-1)- and nuclear factor kappaB (NF-kappaB)-dependent transcriptional events in carcinogenesis. *Free Radic Biol Med* 28: 1338-1348, 2000.
- Brandes RP, Weissmann N and Schröder K: Nox family NADPH oxidases: Molecular mechanisms of activation. *Free Radic Biol Med* 76: 208-226, 2014.
- Cao J, Liu Z, Xu Q, Shi R and Zhang G: Research progress in NADPH oxidase family in cardiovascular diseases. *Zhong Nan Da Xue Xue Bao Yi Xue Ban* 44: 1258-1267, 2019 (In Chinese).
- Sorce S, Stocker R, Seredenina T, Holmdahl R, Aguzzi A, Chio A, Depaulis A, Heitz F, Olofsson P, Olsson T, *et al*: NADPH oxidases as drug targets and biomarkers in neurodegenerative diseases: What is the evidence? *Free Radic Biol Med* 112: 387-396, 2017.
- Makhezer N, Ben Khemis M, Liu D, Khichane Y, Marzaioli V, Tlili A, Mojallali M, Pintard C, Letteron P, Hurtado-Nedelec M, *et al*: NOX1-derived ROS drive the expression of Lipocalin-2 in colonic epithelial cells in inflammatory conditions. *Mucosal Immunol* 12: 117-131, 2019.
- Ward PA and Hunninghake GW: Lung inflammation and fibrosis. *Am J Respir Crit Care Med* 157: S123-S129, 1998.
- Juhász A, Markel S, Gaur S, Liu H, Lu J, Jiang G, Wu X, Antony S, Wu Y, Melillo G, *et al*: NADPH oxidase 1 supports proliferation of colon cancer cells by modulating reactive oxygen species-dependent signal transduction. *J Biol Chem* 292: 7866-7887, 2017.
- Yamamoto T, Nakano H, Shiomi K, Wanibuchi K, Masui H, Takahashi T, Urano Y and Kamata T: Identification and characterization of a novel NADPH oxidase 1 (Nox1) inhibitor that suppresses proliferation of colon and stomach cancer cells. *Biol Pharm Bull* 41: 419-426, 2018.
- Vaquero EC, Edderkaoui M, Pandol SJ, Gukovsky I and Gukovskaya AS: Reactive oxygen species produced by NAD(P)H oxidase inhibit apoptosis in pancreatic cancer cells. *J Biol Chem* 279: 34643-34654, 2004.
- Luxen S, Belinsky SA and Knaus UG: Silencing of DUOX NADPH oxidases by promoter hypermethylation in lung cancer. *Cancer Res* 68: 1037-1045, 2008.
- Höll M, Koziel R, Schäfer G, Pircher H, Pauck A, Hermann M, Klocker H, Jansen-Dürr P and Sampson N: ROS signaling by NADPH oxidase 5 modulates the proliferation and survival of prostate carcinoma cells. *Mol Carcinog* 55: 27-39, 2016.
- Dho SH, Kim JY, Lee KP, Kwon ES, Lim JC, Kim CJ, Jeong D and Kwon KS: STAT5A-mediated NOX5-L expression promotes the proliferation and metastasis of breast cancer cells. *Exp Cell Res* 351: 51-58, 2017.
- Antony S, Jiang G, Wu Y, Meitzler JL, Makhlof HR, Haines DC, Butcher D, Hoon DS, Ji J, Zhang Y, *et al*: NADPH oxidase 5 (NOX5)-induced reactive oxygen signaling modulates normoxic HIF-1 $\alpha$  and p27<sup>Kip1</sup> expression in malignant melanoma and other human tumors. *Mol Carcinog* 56: 2643-2662, 2017.
- Kamiguti AS, Serrander L, Lin K, Harris RJ, Cawley JC, Allsup DJ, Slupsky JR, Krause KH and Zuzel M: Expression and activity of NOX5 in the circulating malignant B cells of hairy cell leukemia. *J Immunol* 175: 8424-8430, 2005.
- Zhou X, Li D, Resnick MB, Wands J and Cao W: NADPH oxidase NOX5-S and nuclear factor  $\kappa$ B1 mediate acid-induced microsomal prostaglandin E synthase-1 expression in Barrett's esophageal adenocarcinoma cells. *Mol Pharmacol* 83: 978-990, 2013.
- Ashizawa N, Shimizu H, Sudo M, Furuya S, Akaike H, Hosomura N, Kawaguchi Y, Amemiya H, Kawaida H, Inoue S, *et al*: Clinical significance of NADPH oxidase 5 in human colon cancer. *Anticancer Res* 39: 4405-4410, 2019.
- Livak KJ and Schmittgen TD: Analysis of relative gene expression data using real-time quantitative PCR and the 2(-Delta Delta C(T)) method. *Methods* 25: 402-408, 2001.
- Maruyama S, Furuya S, Shiraishi K, Shimizu H, Saito R, Akaike H, Hosomura N, Kawaguchi Y, Amemiya H, Kawaida H, *et al*: Inhibition of apoptosis by miR-122-5p in  $\alpha$ -fetoprotein-producing gastric cancer. *Oncol Rep* 41: 2595-2600, 2019.
- Bedard K and Krause KH: The NOX family of ROS-generating NADPH oxidases: Physiology and pathophysiology. *Physiol Rev* 87: 245-313, 2007.
- Laurent E, McCoy JW III, Macina RA, Liu W, Cheng G, Robine S, Papkoff J and Lambeth JD: Nox1 is over-expressed in human colon cancers and correlates with activating mutations in K-Ras. *Int J Cancer* 123: 100-107, 2008.
- Wang HP, Wang X, Gong LF, Chen WJ, Hao Z, Feng SW, Wu YB, Ye T and Cai YK: Nox1 promotes colon cancer cell metastasis via activation of the ADAM17 pathway. *Eur Rev Med Pharmacol Sci* 20: 4474-4481, 2016.
- Fulton DJ: Nox5 and the regulation of cellular function. *Antioxid Redox Signal* 11: 2443-2452, 2009.
- Bánfi B, Molnár G, Maturana A, Steger K, Hegedűs B, Demareux N and Krause KH: A Ca(2+)-activated NADPH oxidase in testis, spleen, and lymph nodes. *J Biol Chem* 276: 37594-37601, 2001.
- Montezano AC, Tsiropoulou S, Dulak-Lis M, Harvey A, Camargo Lde L and Touyz RM: Redox signaling, Nox5 and vascular remodeling in hypertension. *Curr Opin Nephrol Hypertens* 24: 425-433, 2015.
- Holterman CE, Boisvert NC, Thibodeau JF, Kamto E, Novakovic M, Abd-Elrahman KS, Ferguson SSG and Kennedy CRJ: Podocyte NADPH oxidase 5 promotes renal inflammation regulated by the toll-like receptor pathway. *Antioxid Redox Signal* 30: 1817-1830, 2019.
- Marzaioli V, Hurtado-Nedelec M, Pintard C, Tlili A, Marie JC, Monteiro RC, Gougerot-Pocidalo MA, Dang PM and El-Benna J: NOX5 and p22phox are 2 novel regulators of human monocytic differentiation into dendritic cells. *Blood* 130: 1734-1745, 2017.
- Holterman CE, Thibodeau JF and Kennedy CR: NADPH oxidase 5 and renal disease. *Curr Opin Nephrol Hypertens* 24: 81-87, 2015.
- Montezano AC, De Lucca Camargo L, Persson P, Rios FJ, Harvey AP, Anagnostopoulou A, Palacios R, Gandara ACP, Alves-Lopes R, Neves KB, *et al*: NADPH oxidase 5 is a pro-contractile nox isoform and a point of cross-talk for calcium and redox signaling-implications in vascular function. *J Am Heart Assoc* 7: e009388, 2018.
- Hong J, Li D and Cao W: Rho Kinase ROCK2 mediates acid-induced NADPH oxidase NOX5-S expression in human esophageal adenocarcinoma cells. *PLoS One* 11: e0149735, 2016.
- Pandey D and Fulton DJ: Molecular regulation of NADPH oxidase 5 via the MAPK pathway. *Am J Physiol Heart Circ Physiol* 300: H1336-H1344, 2011.
- Zheng CC, Hu HF, Hong P, Zhang QH, Xu WW, He QY and Li B: Significance of integrin-linked kinase (ILK) in tumorigenesis and its potential implication as a biomarker and therapeutic target for human cancer. *Am J Cancer Res* 9: 186-197, 2019.
- Tsoumas D, Nikou S, Giannopoulou E, Champeris Tsaniras S, Sirinian C, Maroulis I, Taraviras S, Zolota V, Kalofonos HP and Bravou V: ILK Expression in colorectal cancer is associated with EMT, cancer stem cell markers and chemoresistance. *Cancer Genomics Proteomics* 15: 127-141, 2018.
- Smith HW and Marshall CJ: Regulation of cell signalling by uPAR. *Nat Rev Mol Cell Biol* 11: 23-36, 2010.
- Collen D and Lijnen HR: Basic and clinical aspects of fibrinolysis and thrombolysis. *Blood* 78: 3114-3124, 1991.
- Halamkova J, Kiss I, Pavlovsky Z, Tomasek J, Jarkovsky J, Cech Z, Tucek S, Hanakova L, Moulis M, Zavrelouva J, *et al*: Clinical significance of the plasminogen activator system in relation to grade of tumor and treatment response in colorectal carcinoma patients. *Neoplasma* 58: 377-385, 2011.

41. Herszényi L, Farinati F, Cardin R, István G, Molnár LD, Hritz I, De Paoli M, Plebani M and Tulassay Z: Tumor marker utility and prognostic relevance of cathepsin B, cathepsin L, urokinase-type plasminogen activator, plasminogen activator inhibitor type-1, CEA and CA 19-9 in colorectal cancer. *BMC Cancer* 8: 194, 2008.
42. Ossowski L and Aguirre-Ghiso JA: Urokinase receptor and integrin partnership: Coordination of signaling for cell adhesion, migration and growth. *Curr Opin Cell Biol* 12: 613-620, 2000.
43. Terada LS and Nwariaku FE: Escaping anoikis through ROS: ANGPTL4 controls integrin signaling through Nox1. *Cancer Cell* 19: 297-299, 2011.
44. Sánchez-Santos A, Martínez-Hernández MG, Contreras-Ramos A, Ortega-Camarillo C and Baiza-Gutman LA: Hyperglycemia-induced mouse trophoblast spreading is mediated by reactive oxygen species. *Mol Reprod Dev* 85: 303-315, 2018.
45. Kim SH, Kim KH, Yoo BC and Ku JL: Induction of LGR5 by H<sub>2</sub>O<sub>2</sub> treatment is associated with cell proliferation via the JNK signaling pathway in colon cancer cells. *Int J Oncol* 41: 1744-1750, 2012.
46. Wu Y, Konaté MM, Lu J, Makhoul H, Chuaqui R, Antony S, Meitzler JL, Difilippantonio MJ, Liu H, Juhasz A, *et al*: IL-4 and IL-17A cooperatively promote hydrogen peroxide production, oxidative DNA damage, and upregulation of dual oxidase 2 in human colon and pancreatic cancer cells. *J Immunol* 203: 2532-2544, 2019.